FLORIDA INTERNATIONAL UNIVERSITY

Miami, Florida

ELASTOGENESIS IN DEVELOPING MURINE AORTIC VALVE

An Undergraduate Honors Thesis submitted in partial fulfillment of the

requirements for the degree of Bachelor of Science

in

BIOLOGICAL SCIENCES

WITH HONORS

by

Beatriz Abdo Abujamra

2019

To: Dr. Steven Oberbauer, Chairperson
Department of Biological Sciences

This Undergraduate Honors Thesis in Biological Sciences, written by Beatriz Abdo Abujamra entitled "Elastogenesis in developing murine aortic valve", is submitted to you in partial fulfillment of the requirements for Undergraduate Honors in Biological ciences. The Biological Sciences Undergraduate Honors Committee and the candidate's research supervisor have read this thesis. We recommend that it be approved.

Dr. Lidia Kos
Honors Research Supervisor

Dr. Walter M. Goldberg, Chairperson.
Undergraduate Honots Committee

Date of Honors Research Presentation: April 15, 2019

This thesis by Beatriz Abdo Abujamra is approved.

r. Steven Oberbauer, Chairperson
Department of Biological Sciences

Florida International University
2019

AKNOWLEDGMENTS

I would like to start by thanking Dr. Lidia Kos, who has been guiding me throughout my academic journey in the United States. Dr. Kos inspires me with her kindness, mentorship, dedication, and altruism. I am forever thankful for her believing in me and giving me the opportunity to be part of her outstanding laboratory team. I would also like to thank Sana Nasim for giving me her time and patience to teach, help, and listen to me throughout this project. I feel honored to have the opportunity to work with her, and foremost to be her friend. Furthermore, I would like to recognize Dr. Xiaoshuang Li, who kindly and patiently allowed me to learn from her, during her last semester at FIU. She provided me with skills that were essential for this study. I extend my appreciation to all my lab members that directly or indirectly assisted me. I do not take any of them for granted and I admire all in both aspects, professionally and personally. I would like to thank Dr. Goldberg who devoted his time to provide me with the tools necessary for this scientific manuscript to come together. I would like to also express gratitude to my family for always supporting my dreams and encouraging me at all times; I could not have come this far without them. Lastly, I would like to recognize my best friend, Fernanda Melegari, for always supporting, cheering, and believing in me.

ABSTRACT

The presence of melanocytes in the aortic valves of mice have shown to be influencing the process of elastogenesis. In humans, this extracellular matrix component provides stability and flexibility for the leaflet to recoil throughout the systolic and diastolic cycles. However, the process of elastin regulation and production has not yet been fully understood. This study described elastin gene expression throughout the development of murine aortic valves. To accomplish that, aortic valves were isolated from mice at embryonic days E12.5, E16.5, E17.5, E18, and E18.5 as well as postnatally at day P11 and adult stages. *In situ* hybridization technique was also performed in order to detect elastin gene expression in a qualitative level. Regarding the *in situ* hybridization, the results were inconclusive. On the other hand, prominent levels of elastin expression were observed at E18. At this point, elastin gene expression exponentially decreased until adulthood, when it stabilizes. These results indicate that the production of elastin occurs quickly during late stages of development and rapidly ceases upon exposed to new postnatal environmental dynamics.

TABLE OF CONTENTS

Committee Approval Letter……………………………...…………………….……………II

Acknowledgments……………………...………………………….………………….III

Abstract………………………………………………...…………….……………….IV

Table of Contents…………………………………………………………………………V

List of Figures and Tables……………………………………………………………..VI

Introduction……………………………………...…………………………….……….1

Materials and Methods…………………………………………………….….…….…6

Results…………………………………………………………...……………….……..…9

Discussion………………………………………………………...……………….…….18

Literature Cited………………………………………………………………………..20

LIST OF FIGURES AND TABLES

Figure 1. Aortic valve anatomy and leaflet composition……………………..………..…5

Figure 2. Sectioning designs………………………………..…………………….………8

Figure 3. Elastin gene expression using RT-qPCR.………………………….……………9

Data Table 1. Changes made from the original RNAscope® Protocol……………………..11

Figure 4. Elastin expression of murine newborn samples………………..…….………..12

Figure 5. Expression of positive and negative controls in murine adult aortic valve……...13

Figure 6. Elastin expression of newborn aortic wall samples……………………..……..14

Figure 7. Murine E14.5 embryo dissection………………………..…………..………15

Figure 8. Photo of a murine E17.5 embryo……………………………………..………15

Figure 9. Photo of murine postnatal stages prior to aortic valve isolation......……………………………………..……………………………..……...16

Figure 10. Photos of murine embryonic stages prior to aortic valve isolation………………17

INTRODUCTION

Cardiovascular diseases are a major cause of death worldwide and account for one in every three deaths in the United States alone (American Heart Association, 2018). The essential components of the cardiovascular system consist of the heart, blood vessels, and blood. Within the heart, there are four valves that are responsible for the unidirectional hemodynamic performance (Rock et al. 2014). The tricuspid and mitral valves are located between the atria and ventricles, whereas the pulmonary valve is positioned between the right ventricle and the pulmonary artery. Lastly, the aortic valve (AoV) is located between the left ventricle and the aorta. During diastole, the valve closes and prevents backflow of blood; during systole, the valve opens and allows blood outflow to be distributed to other organs through the aorta. Hence, the AoV functions within highly oxygenated blood environment and in high-pressure settings. The valve possesses three cusps or leaflets, each of which upon maturity is composed of three layers: the fibrosa, the spongiosa, and the ventricularis, as shown in Figure 1. The fibrosa is the layer facing the aorta and is constituted of collagen, interstitial cells, and a monolayer of endothelial cells. The ventricularis, is the layer facing the ventricle and it consists of elastin and a monolayer of endothelial cells; the rest are interstitial cells. Lastly, the spongiosa, resides in between the other layers and it is composed of interstitial cells, elastin, collagen, and glycosaminoglycans (GAGs) (Angel et al. 2011). These components and their proper organization within each leaflet afford the AoV with its elasticity and mechanical strength traits.

The aortic valve interstitial cells and the extracellular matrix (ECM) are the dominant structural components of the leaflets (Hinton Jr et al. 2006). During valvulogenesis, the ECM is being continuously expanded and remodeled. Its constituents - collagen, elastin, and GAGs

– sustain the integrity of the leaflets throughout the biomechanical valve activity (Schenke-Laylan et al. 2009, Hilton et al. 2006). Overall, valve ECM organization in mice is similar to that of humans, as well as the remodeling process that occurs during development for the formation of a mature adult valve (Hinton et al. 2006). The terminology used for the mouse development are embryonic days (E) and post-natal days (P), while the term for human development is estimated gestational age (EGA) (Krishnan et al 2014). In mice, aortic valvulogenesis begins at embryonic day 9 (E9.0), when the cushions, the precursor structures of the valve leaflets, are formed and cell-to-cell interactions are loosened (Dahal et al. 2017). Throughout cushion elongation (E15.5) the cell density is homogeneous throughout the valve leaflet and the trilaminar structure is not yet established (Hinton et al. 2006). During remodeling (E17), the ECM becomes stratified with different cell densities in each layer, especially in the fibrosa and ventricularis layers (Hinton et al. 2006). The ECM remodeling is a continual process that maintains valve homeostasis after birth, when the leaflets reach maturity and the layers become well defined (Angel et al. 2011).

Disruption or changes in ECM have been reported as the main cause of aortic valve malfunction, leading to common cardiovascular diseases. Currently, there has been no documentation of any cellular treatments for valvular diseases, except for replacement and limited allografts (Schenke-Laylan et al. 2009). Aging is the most likely cause of valvular degeneration, in humans, which causes a significant decrease in the number of interstitial and endothelial cells within the valve (Anstine et al. 2016). Congenital diseases may also result in compromised AoV function. For example, bicuspid aortic valves (BAV) is a connective tissue disease characterized by two thickened leaflets rather than the conventional three, and may result in a narrowed valve, a condition known as AoV stenosis. The AoV stenosis causes

a compensatory effect on the contraction of the heart, which becomes more intense causing murmurs and increasing the risk of AoV rupture (Rose et al. 2018). Recent studies indicate that BAV results from the combination of developmental alterations in the interstitial cells, ECM assembly, and its increased production (Hinton et al. 2006). Aortic stenosis can also be associated with a secondary disease, such as William Syndrome in which one of the elastin alleles is deleted by a genetic mutation, causing major malformations (Ewart et al. 1994).

Elastin (*Eln*) is a non-soluble, stable, and enduring protein that is associated with microfibrillar and linking proteins as well as soluble factors, all of which form elastic fibers (Votteler et al. 2013). These fibers are highly flexible and are located mainly in the ventricularis layer of the AoV (Vesely 1997). Besides providing recoil features to the leaflets during systole and diastole, elastic fibers have a radial arrangement which surrounds and restores collagen into its circumferential configuration, so that both ECM components can accomplish the valve biomechanical cycle (Vesely 1997). This radial configuration of elastic fibers is highly important and dictates the mechanical function of the protein. Throughout early development, elastic fibers are congregated, and erroneous organization or damaged fibers lead to cardiac diseases that could be fatal (Wagenseil et al. 2010). Elastin fiber fragmentation has also been associated to AoV calcification, the foremost cause of valve replacement and heart insufficiency (Votteler et al. 2013). Wagenseil and colleagues investigated the process of elastogenesis in the murine aorta and found that elastin expression appears at E14 and increases until the mouse becomes a neonate. During postnatal stages, elastin expression exponentially decreases until elastin production reaches a plateau that persists during the animal's lifespan (Wagenseil et al. 2010).

Brito and Kos (2008) showed the presence of melanocytes, pigment-producing cells, in murine atrioventricular and aortic valves that lead to their hardening and change in their biomechanical activity. Melanocytes are neural crest-derived cells found mostly in the skin where they provide pigment to keratinocytes as a protective mechanism against ultraviolet radiation. Besides the skin and heart, melanocytes are found in the eyes, meninges, and inner ears (Brito and Kos 2008). The production of melanin, the insoluble pigment molecule, is regulated by the activity of the protein tyrosinase and by other factors such as the microphthalmia-associated transcription factor (Gudjhonsen, et al. 2015). Mouse mutants that lack melanocytes in the skin ($Kit^{w-v/w-v}$) also lack melanocytes in the valve leaflets. Transgenic mice that have hyperpigmented skin and coat (K5-Edn3) also show excessive pigmentation in the valve leaflets (Brito and Kos 2008). Interestingly, two-photon microscopy imaging of leaflets from these mutant mice has shown that $Kit^{w-v/w-v}$ mice have no detectable elastin fibers (unpublished data). These findings suggest that melanocytes may directly or indirectly engage in the process of elastogenesis. Nonetheless, the production of elastin in murine cardiac valves has not yet been investigated. The aim of this study is to establish the timeline of elastogenesis in murine aortic valve by quantifying elastin gene expression throughout prenatal and postnatal stages and to perform an innovative technology of *in situ* hybridization to localize the elastin expression.

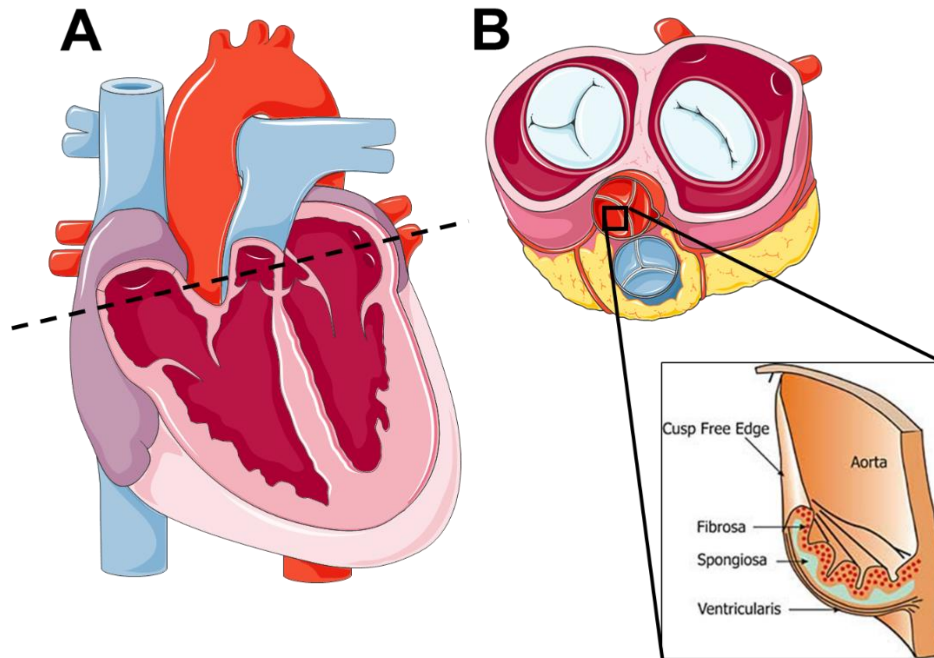

Figure 1. Diagrammatic representation of the human sectioned to show internal anatomy (Rock et al. 2014). (A) Cross-section of the heart to show valve leaflets and (B) leaflet trilaminar structure (boxed area).

MATERIALS AND METHODS

Mice

Wild type mice, C57BL/6J, were obtained from Jackson Laboratory (Bar Harbor, ME). Mice were housed and bred in the Animal Care Facility at Florida International University (Miami, FL, USA). All animal work was approved by the Florida International University Institutional Animal Care and Use Committee and performed according to institutional guidelines established by the National Institutes of Health (Guide for the Care and Use of Laboratory Animals, 2011).

Tissue preparation

Aortic valves were dissected from E12.5, E16.5, E17.5, E18, and E18.5 embryos, 1 and 11 days-old pups and adults (more than 4-weeks-old) using a Leica MZ6 dissecting microscope and fixed in 4% paraformaldehyde (PFA) (Thermo Fisher Scientific, Waltham, MA) overnight. Aortic valves were then washed with PBS and incubated at 4˚C in 10% sucrose for 6 hours, and in 20% sucrose, overnight. Aortic valves were embedded in optimum cutting temperature (OCT) compound for frozen tissue (Thermo Fisher Scientific, Hampton, NH), and immediately frozen at -80°C in order to maintain the desired orientations. Valves were embedded in two different ways shown in Figure 2. In the first orientation, the aortic tube was maintained intact with the leaflets in their natural positions (Figure 2a), and in the second, the tube was cut open longitudinally exposing the leaflets (Figure 2b). A Leica CM3050S cryostat was used to section the samples at 6 µm placed on glass slides in a sequential manner; the sections were then stored at -80°C.

Gene expression Analysis

RNA isolation was performed using the GeneJET RNA Purification Kit (Thermo Fisher Scientific). Total RNA was purified according to the manufacturer's protocol and was eluted in 15 µL of nuclease-free water. RNA was quantified using Thermo Scientific Nanodrop™ 2000 Spectrophotometer. Complementary DNA was synthesized from 15ng of RNA using the RevertAid First Strand cDNA Synthesis Kit (Thermo Scientific). Upon synthesis of cDNA, using the manufacturer's protocol, quantitative real-time polymerase chain reactions (RT-qPCR) were carried out for 40 cycles using the Applied Biosystems™ 7500 system. To accomplish that, the following *Eln* primers were used: 5'GGCTTTGGACTTTCTCCCATT3' and 5'CCGGCCACAGGATTTCC3'. Levels of cDNA were normalized with GAPDH, using primers 5'ATTTGCAGTGGCAAAGTGGAGATTG3' and 5'TGGTTCACACCCATCACAAACATG3'.

In situ Hybridization

Elastin expression in the AoV was assessed using RNAscope® Multiplex Fluorescent Reagent Kit v2 assay (Advanced Cell Diagnostics, ACD, Newark, CA). Briefly, after heating the slides at 40°C for 60 minutes, the sections were post-fixed with 4% PFA for 15 min and then dehydrated. The endogenous enzyme horseradish peroxidase (HRP) was blocked using hydrogen peroxide (1-5%) for 10 mins; slides were then submerged in heated Target Retrieval Reagent for 15 min. After washes in distilled water, the slides were incubated with Protease III at 40°C for 30 min. The *Eln* as well as positive and negative probes were hybridized followed by the addition of HRP-Channel 1, TSA fluorescein (fluorophores), and HRP blocker. The slides were mounted with RNAscope® Multiplex Fluorescent Reagent Kit

v2 DAPI (Advanced Cell Diagnostics, Newark, CA) and the images were captured with Olympus Confocal BX61 microscope; image analysis was performed using Image J.

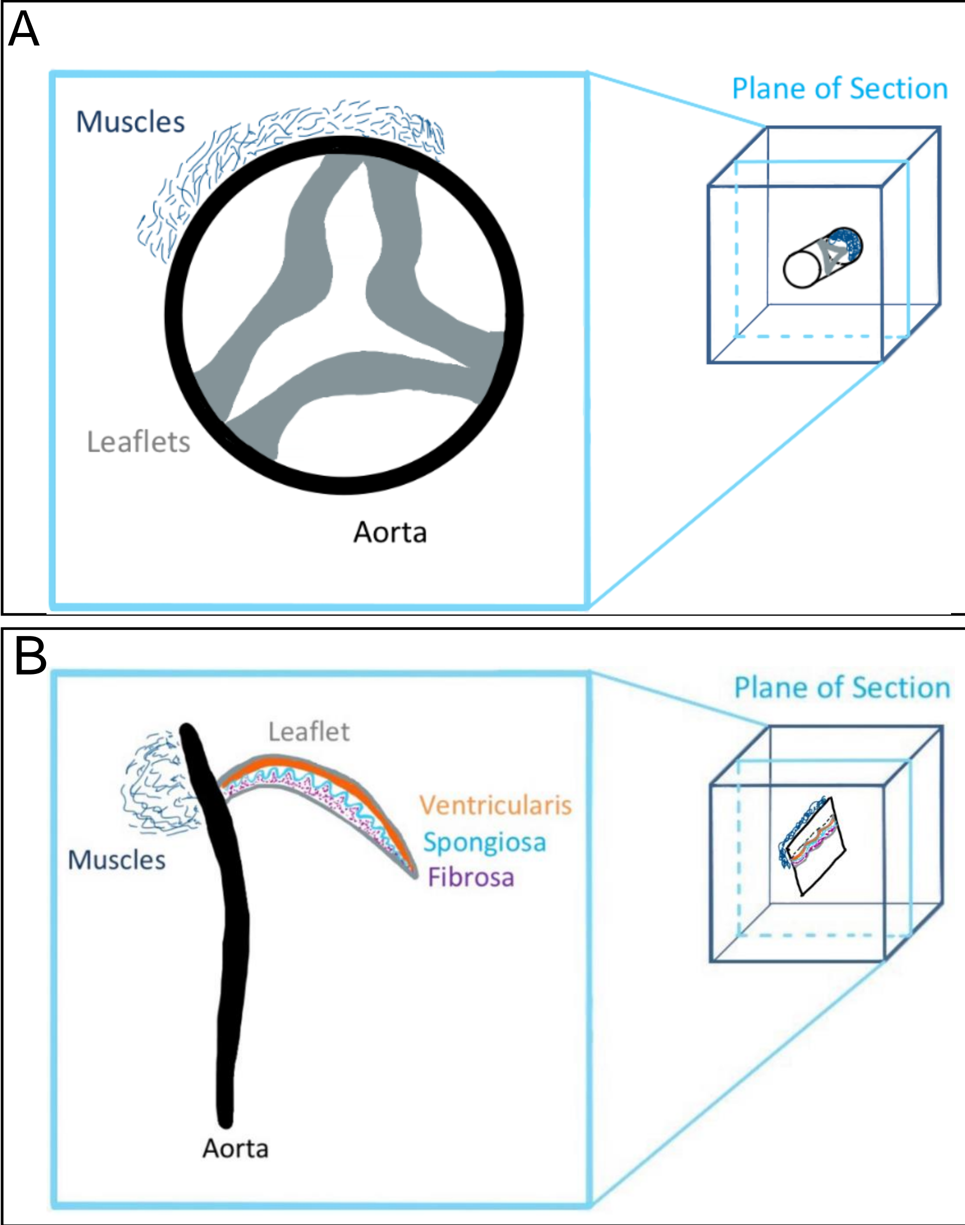

Figure 2. Sectioning methods allowing different analysis of the AoV leaflets. (A) corresponds to the orientation of the closed aorta facing the oberserver, that is also the side to be sectioned. The leaflets are located at the bottom of the tissue. (B) represents the orientation of the opened aorta facing the sectioning plane. In this way, the leaflets are facing the side of the OCT disposable mold.

RESULTS

Elastin expression in the AoV

In order to establish the timing of expression of elastin (*Eln*) in the murine aortic valve, I performed RT-qPCR at various embryonic and postnatal stages. At E12.5, prior to the major phase of cushion elongation, elastin is expressed at incredibly low levels. As elongation and remodeling start to occur, *Eln* levels increase gradually and reach a peak at E18. After this time, expression decreases back to the levels found at E12.5, becoming even lower in adulthood (Figure 3).

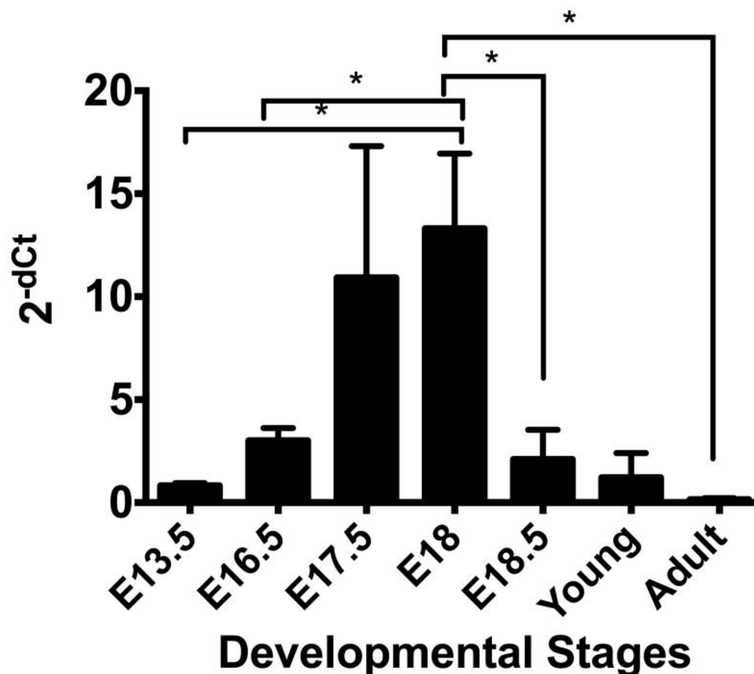

Figure 3. RT-qPCR analysis of *Eln* expression on murine AoV. Aortic valves were isolated, and levels of expression were compared distinct stages: E12.5, E16.5, E17.5, E18, and E18.5 as well as postnatal day P11, and adult stage (n=4-5/stage).

Spatial localization of elastin expression in the AoV

To further characterize *Eln* expression in the AoV and establish which cell type is responsible for its production during valvulogenesis, I attempted to perform *in situ* hybridization using the RNAscope assay. My first attempt was with leaflets at the newborn (P1) stage using the

exact protocol provided by the manufacturer. Fluorescence was detected throughout the leaflet, particularly at the edges, but the pattern observed (Figure 4) did not correspond to the characteristic punctuated images obtained with this technique. As such, and upon recommendations from the manufacturer, the protocol was re-evaluated to ensure that the tissue was properly handled and to prevent RNA degradation. The changes made from the original protocol for each subsequent trial, including temperature, fixation, fluorophore dilution, and target retrieval are presented in Table 1.

Subsequently, to determine whether the protocol was the main issue, the ubiquitin C gene (UBC) that is highly expressed in the heart was used as a positive control. By contrast, the RNA polymerase II subunit A (POLR2A), one that is not as expressed in adult aortic valve, was used as a negative control. Both of these were provided by the RNAscope®. Figure 5 demonstrates that although there is no significant expression of both genes, the technique worked as anticipated in the adult aortic valve. This result suggests that RNA degradation may be the main cause of the failed experiments.

Changes were made in the dissection protocol as well as RNAscope protocol (Table 1) of the newborn mouse aortic wall to analyze elastin expression and account for sample degradation. Elastin expression was detected throughout the aortic tissue as expected (Figure 6). The protocol was thereby finalized in order to address the aortic valve specific characteristics, such as tissue size, elastin expression, and rapid RNA degradation. In this way, the three developing stages can be studied more accurately.

Table 1. Changes made from the original RNAscope® for tissue sample optimization.

Steps	Changes 1 Trial #1	Changes 2 Trial #2	Changes 3 Trial #3
Warming the slides	Slides were warmed for 1 hour at 40°C	Slides were warmed for 30 min at 60°C	Slides were warmed for 1 hour at 40°C
Post-fixing the samples	Post fixed the samples in 4% PFA for 15 mins at 4°C	Post fixed the samples in 4% PFA for 15 mins at room temperature	Post fixed the samples in 4% PFA for 15 mins at 4°C
Target Retrieval (heat-induced antigen retrieval to reverse cross-linking as a result of post-fixation)	No change from original protocol	No change from original protocol	Slides were boiled (98/102°C) in target retrieval solution for 5 minutes
Fluorophore dilution	TSA Plus Fluorophore dilution was made from 1:1500 to 1:750	TSA Plus Fluorophore dilution was made from 1:1500 to 1:750	TSA Plus Fluorophore dilution was made from 1:1500 to 1:750
Results	**Figure 4**	**Figure 5**	**Figure 6**

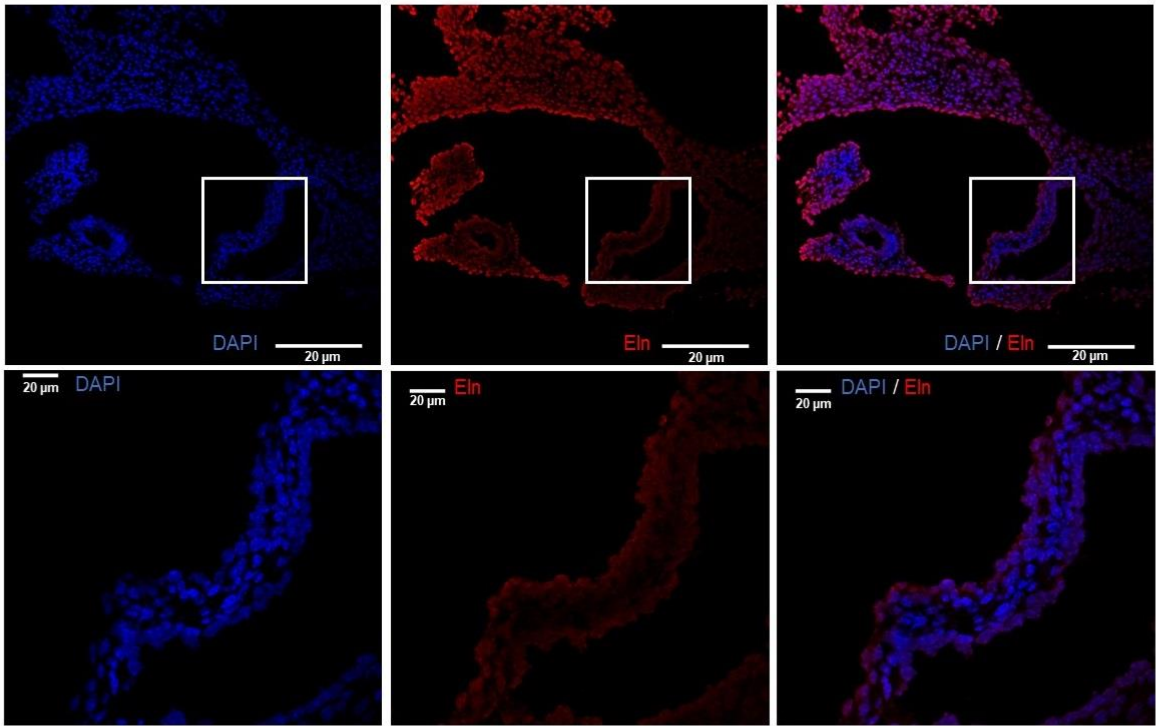
A
DAPI
20 µm
Eln
20 µm
DAPI / Eln
20 µm
20 µm
DAPI
20 µm
Eln
20 µm
DAPI / Eln

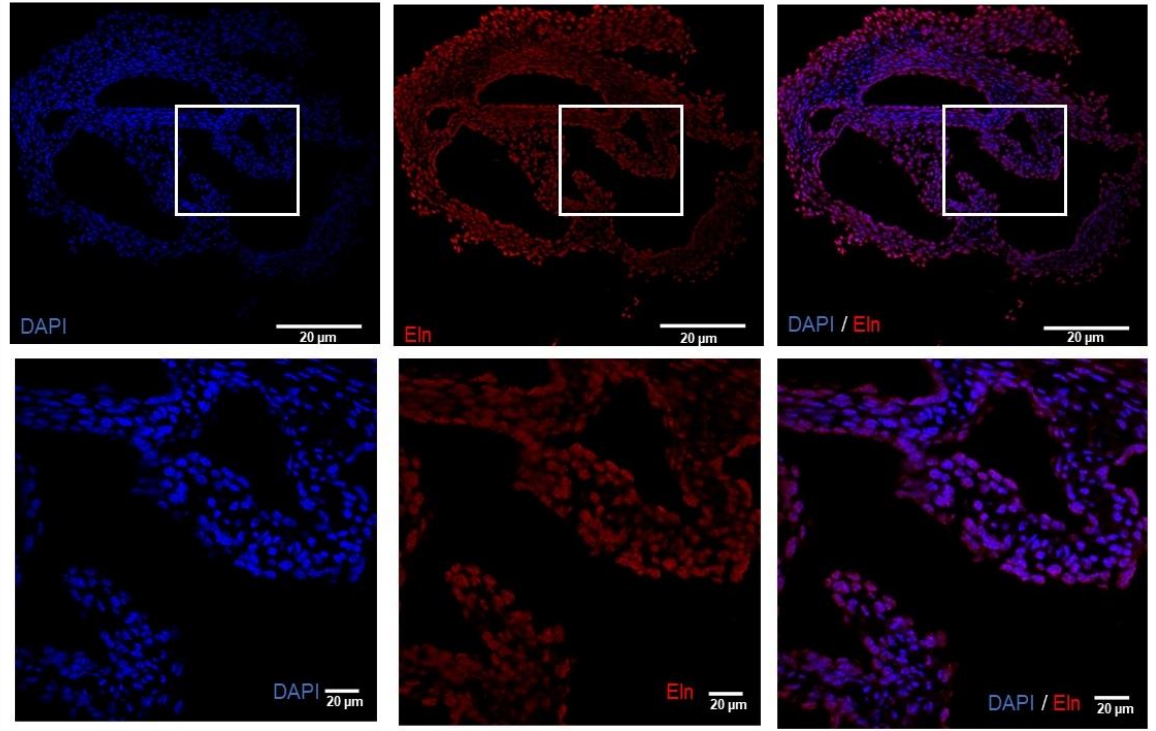
B
DAPI
20 µm
Eln
20 µm
DAPI / Eln
20 µm
DAPI
20 µm
Eln
20 µm
DAPI / Eln
20 µm

Figure 4. *Eln* (red) expression of two murine newborn samples (A, B). Results did not relate to punctuated dots, as expected. Cell nuclei are stained with DAPI (blue). The boxed areas of the 20X figures correspond to the leaflets that are shown in higher magnification (60X) on the rows below. Sections were analyzed using a confocal microscope.

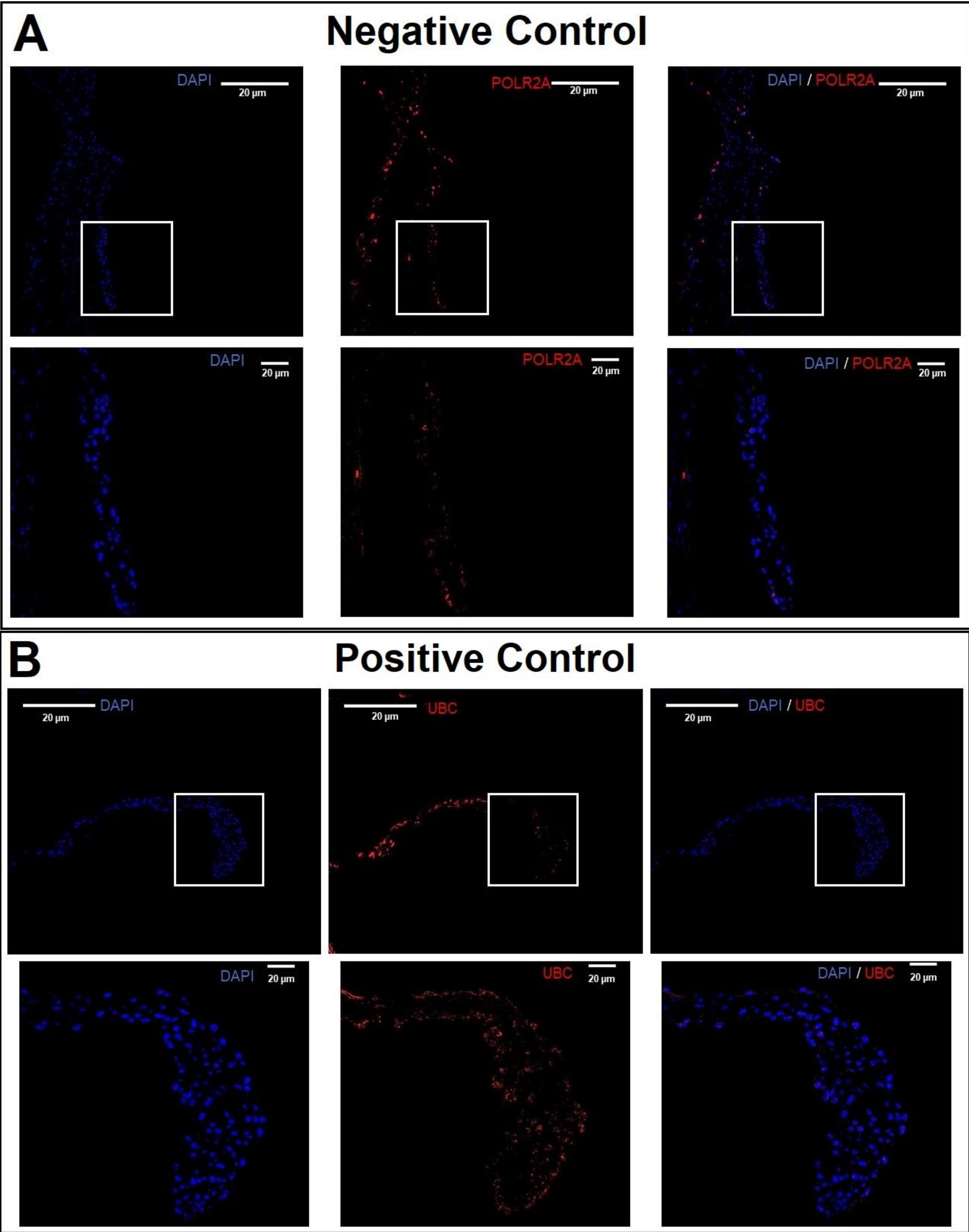

Figure 5. Expression of a positive and negative control in murine adult aortic valve. Images analyzed using a confocal microscope show that the negative control probe (A) has a lower expression as compared to positive control probe (B). The lower row in A and B represents the magnified (60X) boxed area.

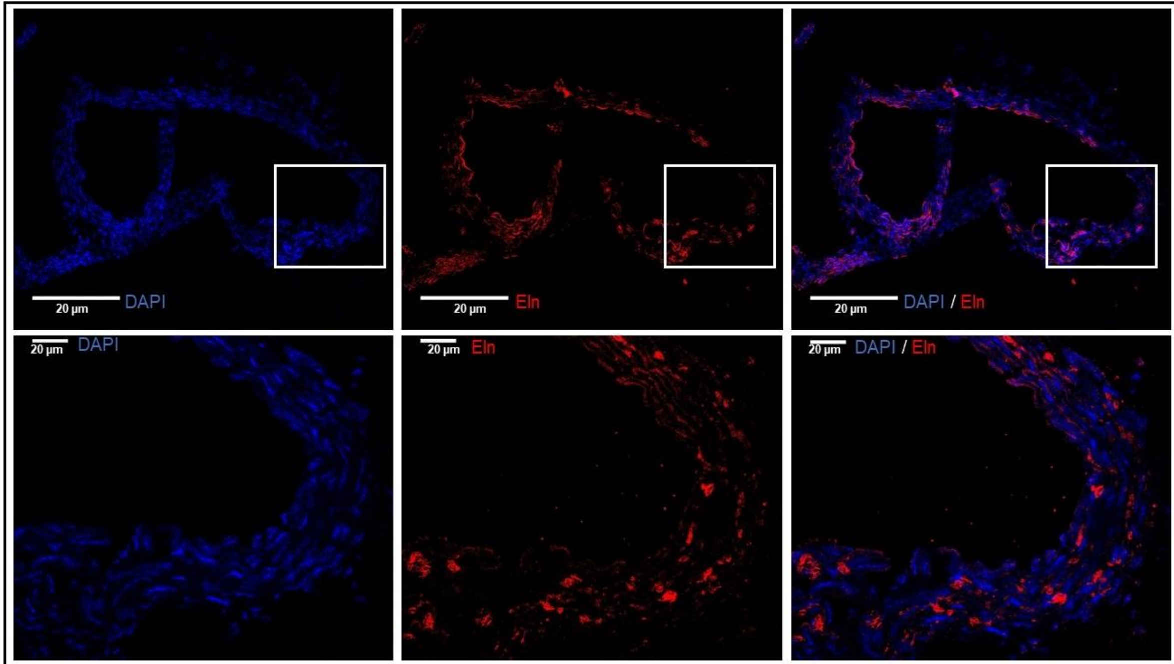

Figure 6. Section of a newborn aortic wall visualized under a confocal microscope shows the pattern of elastin expression labeled in red, and cellular nuclei in blue. The first row corresponds to the aorta at 20X magnification, while the second row represents the magnified boxed area at 60X.

Macroscopic analysis of embryos and neonate mice

Concomitantly to RNAscope protocol optimization, the aortic valve of E14.5, E17.5 embryos, and neonate (P1) were isolated as shown in Figures 7-9.

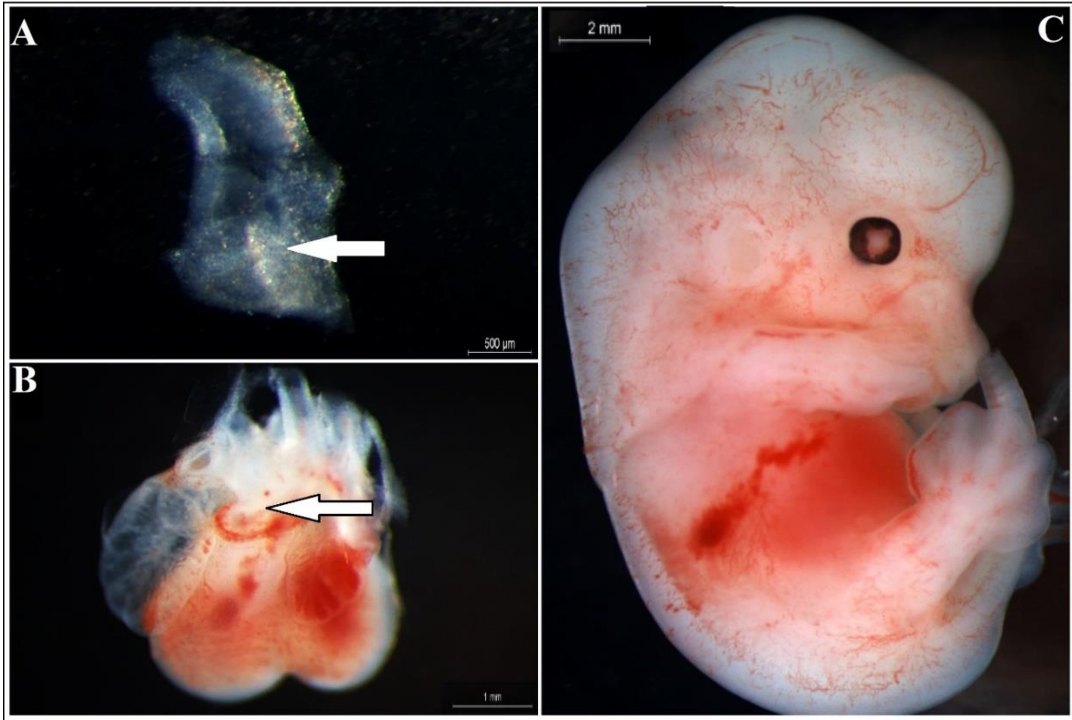

Figure 7. Murine E14.5 embryo dissection. (A) shows the aorta containing the three leaflets (arrow). (B) shows the heart of the embryo containing the aorta (arrow). (C) represents the entire E14.5 embryo.

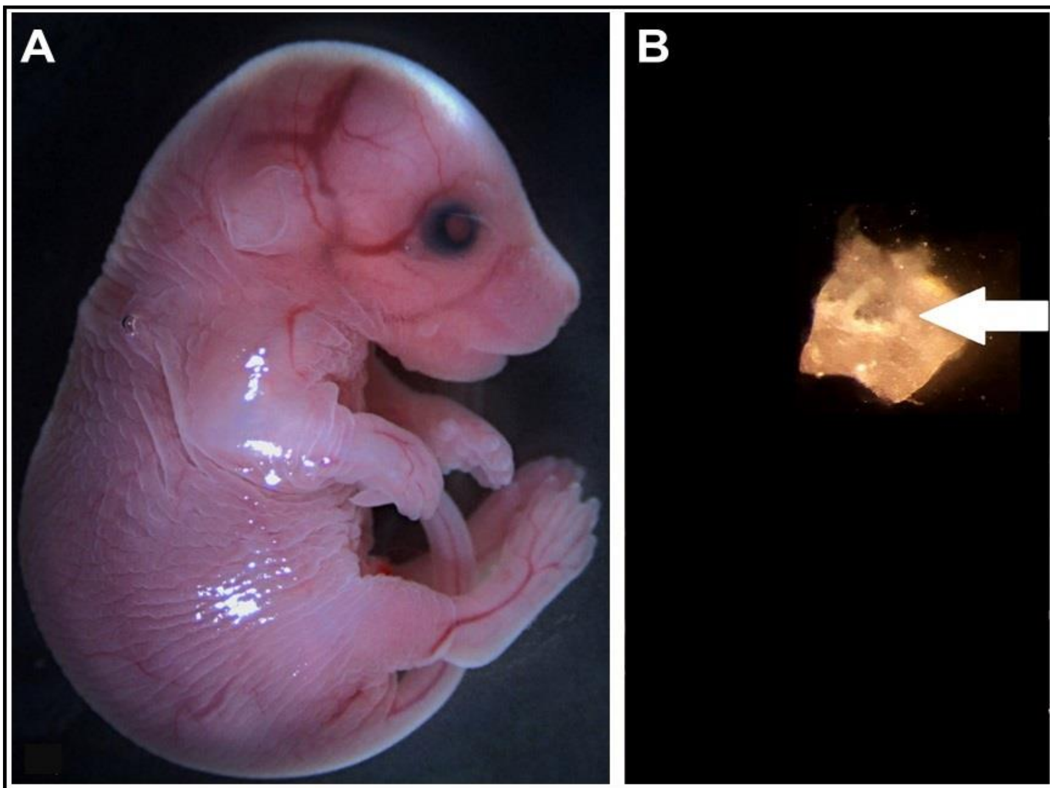

Figure 8. Photo of a murine E17.5 embryo. (A) corresponds to the embryo prior to dissection, whereas (B) illustrates the aorta containing the developing aortic valve (arrow).

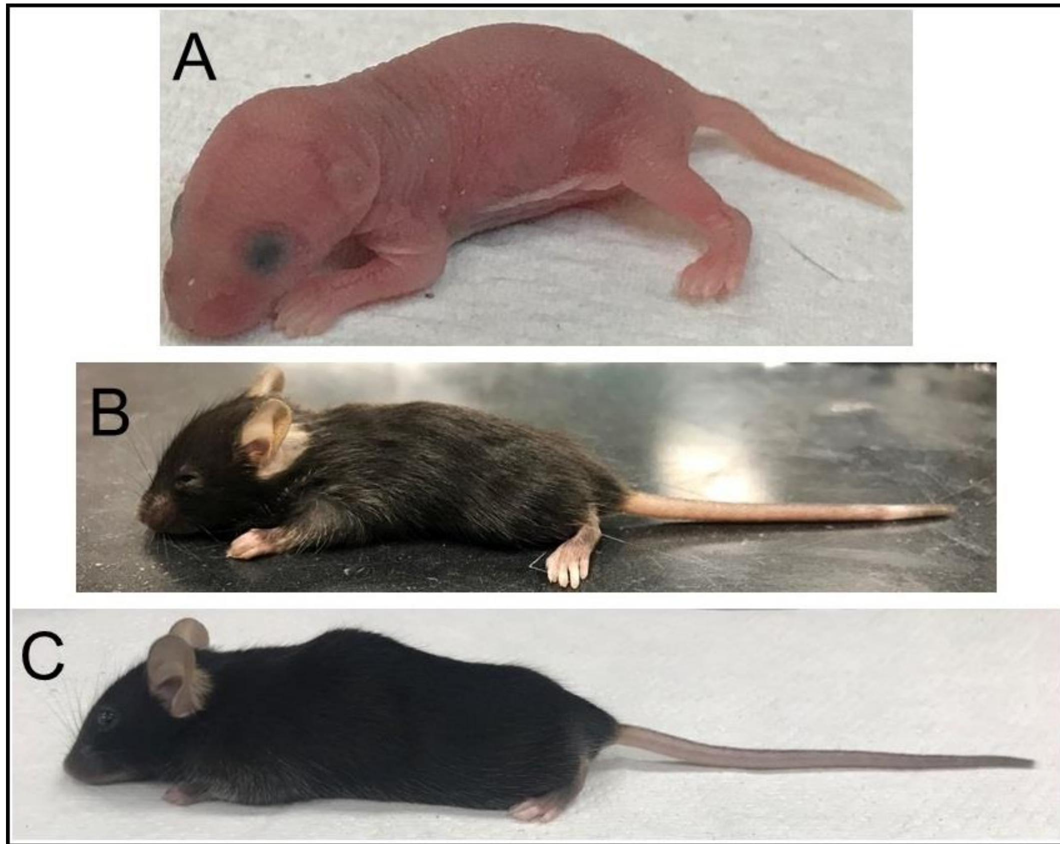

Figure 9. Murine at postnatal stages prior to aortic valve isolation. (A) corresponds to newborn P1, while (B) represents a young stage P11, and (C) shows an adult, greater than four weeks-old.

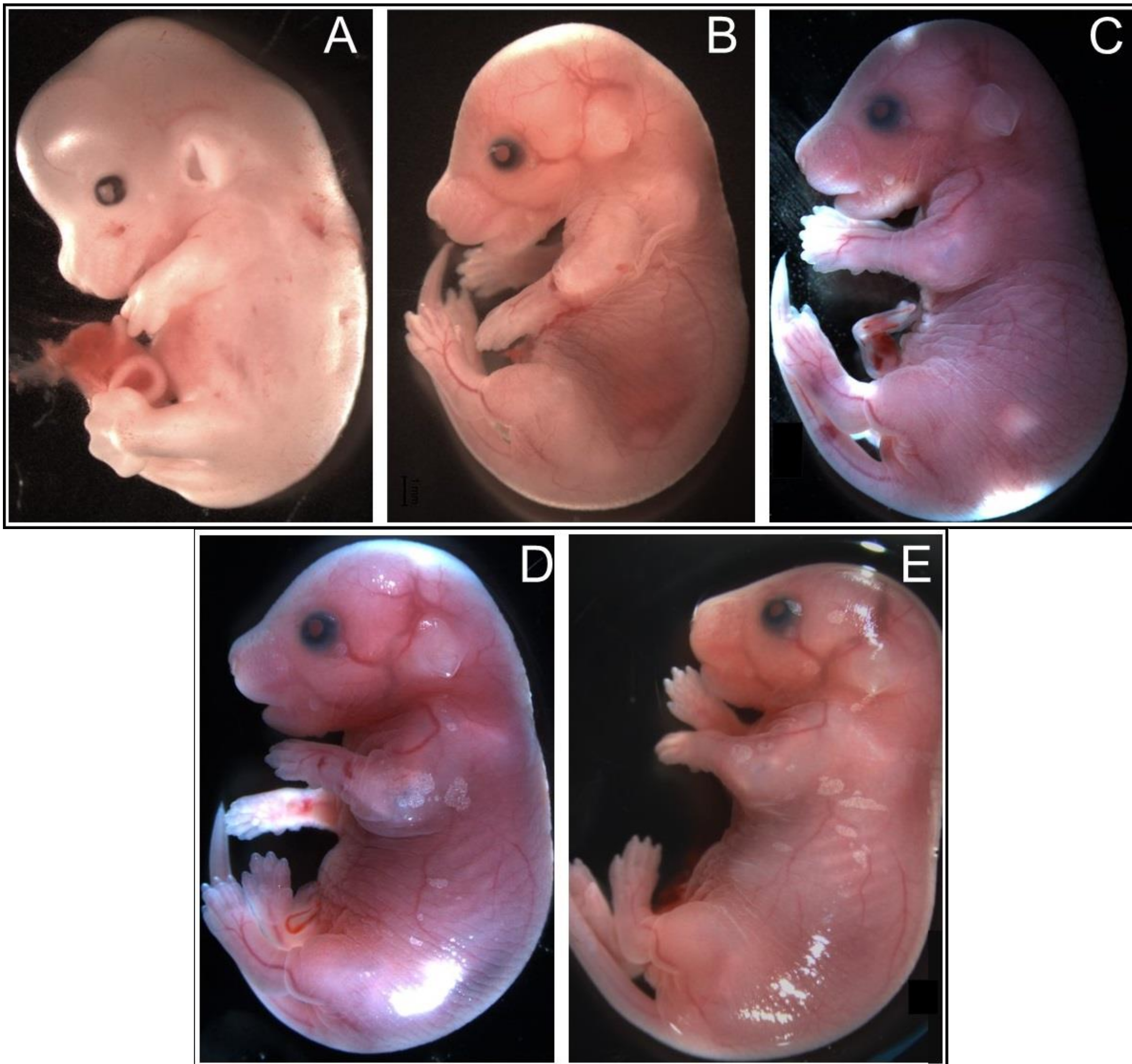

Figure 10. Murine embryos at different developmental stages obtained for this study, preceding AoV isolation. Embryos at embryonic day (A) E12.5, (B) E16.5, (C) E17.5, (D) E18, and (E) E18.5.

DISCUSSION

This is the first study that has investigated elastin gene expression in murine aortic valve at the mRNA level throughout various stages of development. The only other study that has described the process of elastogenesis at the molecular level was carried out in the human aortic valve leaflets (Votteler et al. 2013). They showed that tropoelastin, a soluble precursor of elastin, expression begins at the start of valve development when the heartbeat is first detected, corresponding to week four of pregnancy. Three weeks later, at Estimated Gestational Age 7, *Eln* expression is at its peak when the leaflets are emerging from the reorganization of the cushions, then the gene expression and production significantly decreases until adulthood (Votteler et al. 2013). Despite this low level of gene expression, elastic fibers are abundant in the ventricularis layer of an adult AoV leaflet, evidencing the long durability of elastin proteins (Votteler et al. 2013). Therefore, elastin production accompanies the maturation process of the valves and the heart, and it is influenced by the local environmental forces that impinge on the leaflets. The results obtained from the RT-qPCR does not corroborate the pattern of *Eln* expression seen in humans. It was found that late embryonic stages of murine AoV have higher expression than in the early stages and postnatal stages. The peak of gene expression in murine AoV is at E18, which has no comparable week with humans (Krishnan et al. 2013) but it comprehends the second trimester of pregnancy, and it significantly decreases at P11 and adult stages.

In order to spatially localize *Eln* gene expression in the AoV leaflets, RNAscope® was used. It is a more sensitive and specific technology of in situ hybridization as a result of their "double Z" probe design and advanced signal amplification. This assay leads to the detection of a single RNA transcript, which can be visualized as a punctuated dot signal, hence this technique provides understanding of *Eln* gene expression in different cell subpopulations and

tissue samples at the molecule level. Unfortunately, initial results following the protocol provided by the manufacturer were not successful due to RNA degradation and the antigen target retrieval step. The latter is a boiling step of the pretreatment part of the protocol responsible for unmasking the target RNA by reducing the cross-link between protein amino acid residues formed after fixing the samples. Espinosa, et al. (2018) examined elastin mRNA expression in reduced embryonic blood flow in the aorta by using vitelline vein ligation in a chicken. To accomplish their goal, they performed similar *in situ* hybridization technique, RNAscope®. The pattern of their results is similar to the one shown in this study after the last changes in the protocol, where the optimized technique was successfully performed in the murine aortic wall.

Here, insights were provided on the process of elastogenesis in murine aortic valve. Although the profile of *Eln* gene expression has been described and compared with the pattern seen in the human leaflets, further investigation on the spatial localization of this expression needs to be addressed. After troubleshooting the RNAscope® protocol, it is now fully optimized to detect *Eln* expression among the layers of the leaflets at different stages of AoV development, embryonically and postnatally. Further study in combination with *in situ* hybridization, immunofluorescence staining of melanocytic and valve interstitial cells markers, such as tyrosinase and α-smooth muscle actin respectively, will contribute to determining which cell type is regulating or producing elastin in a non-autonomous manner.

LITERATURE CITED

American Heart Association Council on Epidemiology and Prevention Statistics Committee and Stroke Statistics Subcommittee. Heart disease and stroke statistics 2018 update: a report from the American Heart Association https://www.ahajournals.org/doi/10.1161/CIR.0000000000000558

Angel PM, Nusinow D, Brown CB et al. 2011. Networked-based characterization of extracellular matrix proteins from adult mouse pulmonary and aortic valves. Journal of Proteome Research 10: 812-823 doi:10.1021/pr1009806

Anstine LJ, Bobba C, Ghadiali S, Lincoln J. 2016. Growth and maturation of heart valves leads to changes in endothelial cell distribution, impaired function, decreased metabolism and reduced cell proliferation. Journal of Molecular and Cellular Cardiology 100: 72-82. doi: 10.1016/j.yjmcc.2016.10.006

Brito FC, Kos L. 2008. Timeline and distribution of melanocyte precursors in the mouse heart. Pigment Cell & Melanoma Research 21: 464-470. doi:10.1111/j.1755-148X.2008. 00459.

Dahal S, Huang P, Murray BT, Mahler GJ. 2017. Endothelial to mesenchymal transformation is induced by altered extracellular matrix in aortic valve endothelial cells. Journal of Biomedical Materials Research Part A, 105: 2729-2741. doi:10.1002/jbm.a.36133

Espinosa MG, Taber LA, Wagenseil JE. (2018). Reduced embryonic blood flow impacts extracellular matrix deposition in the maturing aorta. Developmental Dynamics 247: 914-923. doi:10.1002/dvdy.24635

Ewart AK, Jin W, Atkinson D et al. 1993. Supravalvula Aortic Stenosis Associated with A Deletion Disrupting the Elastin Gene. Clinical Endocrinology 89: 4-94. doi:10.1111/cen.13727

Gudjohnsen SAH, Atacho DAM, Gesbert F et al. 2015. Meningeal melanocytes in the mouse: Distribution and dependence on *mitf*. Frontiers in Neuroanatomy 9:149. doi:10.3389/fnana.2015.00149

Hinton RB Jr, Lincoln J, Deutsch GH, et al. 2006. Extracellular matrix remodeling and organization in developing and diseased aortic valves. Circulation Research 98: 1431-1438. doi: 10.1161/01.RES.0000224114.65109.4e

Krishnan A, Samtani R, Dhanantwari P et al. 2014. A detailed comparison of mouse and human cardiac development. Pediatric Research 76: 500-507. doi:10.1038/pr.2014.12

Rock CA, Han L, Doehring TC (2014) Complex collagen fiber and membrane morphologies of the whole porcine aortic valve. PLoS ONE 9: e86087. doi: 10.1371/journal.pone.0086087

Rose M, Rigsby C, Berhane H, et al. 2019. 4-D flow MRI aortic 3-D hemodynamics and wall shear stress remain stable over short-term follow-up in pediatric and young adult patients with bicuspid aortic valve. Pediatric Radiology 49: 57-67. doi:10.1007/s00247-018-4257-y

Schenke-Layland K, Stock U A, Nsair A, et al. 2009. Cardiomyopathy is associated with structural remodelling of heart valve extracellular matrix. European Heart Journal 30: 2254-2265. doi:10.1093/eurheartj/ehp267

Vesely I. 1997. The role of elastin in aortic valve mechanics. Journal of Biomechanics 31: 115-123. doi:10.1016/S0021-9290(97)00122-X

Votteler M, Berrio DAC, Horke A et al. 2013. Elastogenesis at the onset of human cardiac valve development. Development 140: 2345-2353. doi:10.1242/dev.093500

Wagenseil JE, Ciliberto CH, Knutsen RH et al. 2010. The importance of elastin to aortic development in mice. American Journal of Physiology - Heart and Circulatory Physiology 299: 257-264. doi:10.1152/ajpheart.00194.2010